Available online at www.sciencedirect.com
SCIENCE DIRECT®
ELSEVIER
Dyes and Pigments 71 (2006) 37–42
DYES and PIGMENTS
www.elsevier.com/locate/dyepig

Preparation, morphological and thermal stability of polyimide/silica hybrid material containing dye NBDPA

Fengxian Qiu [a], Yuming Zhou [b,*], Juzheng Liu [b], Xuping Zhang [c]

[a] School of Chemistry and Chemical Engineering, Jiangsu University, Zhenjiang 212013, China
[b] Department of Chemistry and Chemical Engineering, Southeast University, Nanjing 210096, China
[c] Institute of Optical Communication Engineering, Nanjing University, Nanjing 210093, China

Received 4 October 2004; received in revised form 22 February 2005; accepted 25 May 2005
Available online 9 August 2005

Abstract

In this study, two series of the polyamide/silica NLO hybrid composites with covalent links between the inorganic and the organic networks were synthesized by the sol–gel method. These polyimide hybrid waveguide materials were prepared using a commercially available, 4,4′-(hexafluoro-isopropylidene)diphthalic arhydride (6FDA) or pyromellitic dianhydride (PMDA) as dianhydride, *N*-methyl-*N*-[4-[(6-nitrobenzothiazol-2-yl)diazenyl]phenyl]-2-aminoethano (NBDPA) as NLO-chain dye chromophore, 3-aminopropyltriethoxysilane (APTES) as a coupling agent between the organic and inorganic phase, and a metal alkoxide tetraethylorthosilicate (TEOS). The TEOS content in the hybrid films was varied from 0 to 22.5 wt%. The prepared polyimide/silica hybrids were characterized by IR, thermogravimetric analysis (TGA), X-ray diffraction (XRD), scanning electron microscopy (SEM), transmission electron microscopy (TEM), etc. They exhibited fairly good optical transparency. The SiO_2 phase was well dispersed in the polymer matrix. DSC and TGA results showed that these hybrid materials had excellent thermal stability. The refractive index decreased linearly with the increasing TEOS fraction in the hybrid films. The experimental results suggested that the hybrid thin films had potential applications as passive films for optical devices.

Keywords: Nonlinear optical (NLO); Polyimides; Hybrid

1. Introduction

The photonic technology appears to be an indispensable part of life in 21st century. Nonlinear optical (NLO) materials are key elements for future photonic technologies [1] of optical communication, optical interconnect, oscillator, amplifier, frequency converter, etc. Research on significant effects are being made for the selection of materials showing large NLO susceptibility [2,3]. Extensive studies have been made for the synthesis of nonlinear optical (NLO) materials based on organic compounds over the past decade because of their potential applications in the field of telecommunications, optical signal processing, optical switching, etc. Among the organic materials, the NLO polymers are considered promising materials, mainly because they offer many advantages such as mechanical endurance, light weight, chemical resistance and good processability to form optical devices [4–6]. Polyimide (PI) has been the topic of intensive studies due to its outstanding characteristics such as good chemical and mechanical properties as well as low dielectric constant [7,8]. But most of the polyimides have either low T_g or exhibit poor reproducibility of optical quality including high optical loss which limit their applications as optical devices [9]. Such problems can be alleviated by

---

* Corresponding author. Tel.: +86 2583791274.
E-mail addresses: fxqiuchem@163.com (F. Qiu), ymzhouchem@163.com (Y. Zhou).

0143-7208/$ - see front matter © 2005 Elsevier Ltd. All rights reserved.
doi:10.1016/j.dyepig.2005.05.009

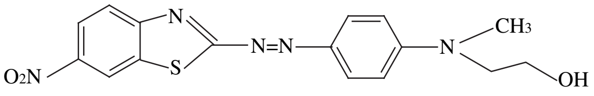

Fig. 1. Chemical structure of the NLO chromophore NBDPA.

approaches such as the sol–gel method and intercalation which introduces various inorganic components into polyimides to obtain inorganic/polyimide hybrids [10–12]. The key challenge for preparation of the hybrid materials is how to control the phase separation between the organic and inorganic moieties. The phase behavior is connected with the interaction between the organic segment and the inorganic network in the hybrids. Hydrogen bonding or covalent bonding is usually used to prevent phase separation [13–15]. On the other hand, SiO_2 has remarkably high thermal stability and its introduction may improve the thermal stability and the adhesion of the composite with the substrate [16]. If the size of SiO_2 composite particles is well controlled, their introduction may not pose great reverse influence upon the photolithographic behavior of the photosensitive PI [17].

In this study, we synthesized two series of polyimide-based NLO waveguide materials containing dye NLO chromophores *N*-methyl-*N*-[4-[(6-nitrobenzothiazol-2-yl)diazenyl]phenyl]-2-aminoethano (NBDPA, made by us, see Fig. 1). When reacted with 3-aminopropyltriethoxysilane, APTES, coupling agent, the functional groups provided a link between the inorganic domains and the polymer matrix. Then, the hybrids were prepared, utilizing organic polymers functionalized with trialkoxysilane group's alkoxysilane monomers containing functional groups that could induce the introduction of chemical bonds between the organic and inorganic phases (Fig. 2). We reported detailed studies

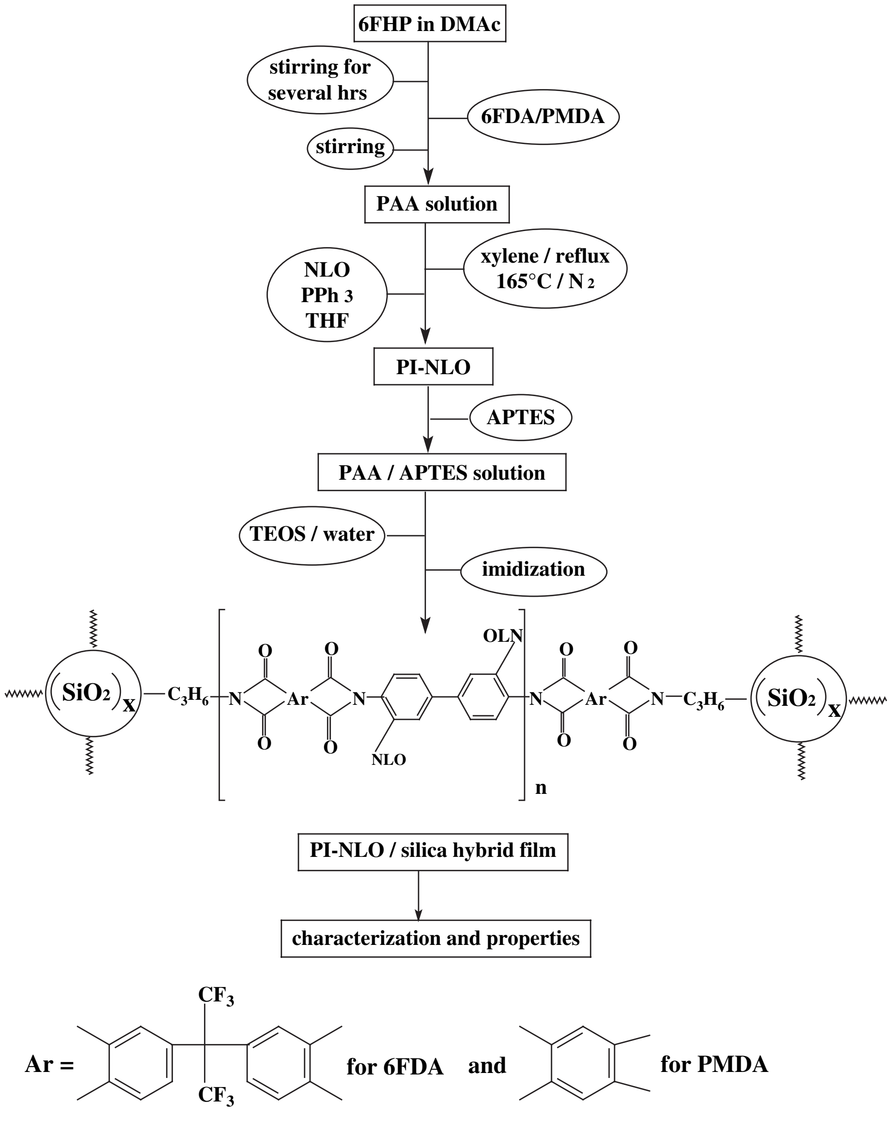

Fig. 2. Reaction scheme for preparing NLO polyamide/silica hybrid materials, FB and PB.

on the characterization of the hybrids, as well as their optical properties, micrographs studies and thermal properties, etc.

2. Experimental

N,*N*-dimethylacetamide (DMAC) was stirred over powered calcium hydride overnight and then distilled under reduced pressure and stored over 4 Å molecular sieves. The 4,4′-(hexafluoro-isopropylidene)diphthalic arhydride (6FDA) and 2,2-bis(3-amino-4-hydroxyphenyl) hexafluoropropane (6FHP) used in the polyimide synthesis were obtained from TCI and used without further purification. The pyromellitic dianhydride (PMDA) was obtained from Beijing chemistry agent plant. The 3-aminopropyltriethoxysilane, APTES was purchased from Nanjing shuguang chemical plant. Tetrahydrofuran (THF) was purified by distillation and other reagents and solvents were obtained commercially and were used as received.

2.1. Preparation of polyimide/SiO_2 hybrid materials (series of FB and PB)

The polymerization was conducted in a dry nitrogen flushed three-neck flask with a magnetic stirrer, reverse Dean-stark trap, and reflux condenser filled dry xylene. A stoichiometric amount of 6FDA (3.3318 g, 7.5 mmol) or PMDA (1.636 g, 7.5 mmol) was added to a solution of 6FHP (2.7470 g, 7.5 mmol) in 30 ml DMAC at 0 °C. The solution was then warmed to room temperature and magnetically stirred overnight under nitrogen. PPh_3 (0.3930 g, 1.5 mmol) and *N*-methyl-*N*-[4-[(6-nitrobenzothiazol-2-yl)diazenyl]phenyl]-2-aminoethano (NBDPA, dye NLO chromophore) (0.5355 g, 1.50 mmol) were dissolved in THF (15 ml) and added dropwise into the solution. The reaction mixture was stirred for 2 days at room temperature. Then, APTES was added and reacted for 4 h. Various contents of TEOS were added as shown in Table 1. After 12 h of reaction, homogeneous transparent sol can be obtained. Then the resulting homogeneous solution was transferred to a conical flask and was sealed with plastic film. After drying for 5 days several small holes were opened for the slow evaporation of the solvent. The homogeneous transparent gel was formed. Then the sample was heated at 110 °C under vacuum for 2 h to remove residual solvent and by-products (water and alcohol, etc.). The thermally stable sol–gel hybrid materials were obtained. The film was spin-coated on a cleaned glass substrate and dried subsequently at 200 °C, for 3 h in air. The synthetic route was shown in Fig. 2.

2.2. Characterization of polyimide/SiO_2 hybrid materials

IR spectra of the prepared thin films were obtained on a KBr pellet using Nicolet AVATAR 360 spectrometer. To examine the optical characteristics of materials with addition of sample light transmission was measured in ultraviolet and visible range by means of spectrophotometer (Shimadzu UV-240). The fracture surfaces of hybrid thin films were examined on the SIRION Scanning Electron Microscope (SEM). HITACHI H-600 Transmission Electron Microscope (TEM) measured the particle sizes. Thermogravimetric analysis (TGA) and differential scanning calorimetry (DSC) were performed on NETZSCH STA449C. The programmed heating range was from room temperature to 800 °C, at a heating rate of 10 °C/min under nitrogen atmosphere. The measurement was taken using 6–10 mg samples. TGA and DSC curves were recorded. X-ray diffraction (XRD) patterns of SiO_2 were obtained with a CuKα X-ray source and a step of 0.02(2θ) and run from $2\theta = 6–80°$ at room temperature.

Table 1
Reactant summary and properties of hybrid materials

Hybrid material	Dianhydride	TEOS (wt%)	APTES (ml)	HCl (ml)	H_2O (ml)	THF (ml)	T_g[a] (°C)	T_d[b] (°C)	$n_{633\ nm}$[c]	Appearance[d]
FB-1	6FDA	5	0.20	0.10	0.25	30	360	505	1.493	Transparent
FB-2	6FDA	10	0.20	0.25	0.53	30	362	510	1.475	Transparent
FB-3	6FDA	15	0.20	0.50	1.02	30	369	512	1.455	Transparent
FB-4	6FDA	22.5	0.20	0.65	2.10	30	370	515	1.414	Semi-transparent
PB-1	PMDA	5	0.20	0.10	0.25	30	352	500	1.525	Transparent
PB-2	PMDA	10	0.20	0.25	0.53	30	357	508	1.491	Transparent
PB-3	PMDA	15	0.20	0.50	1.02	30	361	510	1.462	Transparent
PB-4	PMDA	22.5	0.20	0.65	2.10	30	369	512	1.423	Semi-transparent

[a] Experimental results from DSC.
[b] Experimental results from TGA.
[c] *n* is the refractive index of the prepared thin films.
[d] UV–vis spectrum was observed.

3. Results and discussion

Fig. 3 illustrated the FT-IR spectra of the prepared polyamide/silica hybrid thin films FB-1, FB-3, PB-1 and PB-3. From the spectra, it was noted that the peaks of the characteristic imide absorption were at 729, 1378, 1722, 1786 cm^{-1}. The absorption band around 1055–1150 cm^{-1} gradually increased intensity with increasing silica content, consisted with the formation of the three-dimensional Si–O–Si network in the hybrid film [18,19]. The broad absorption around 3100–3300 cm^{-1} was assigned to the Si–OH residue, formed on hydrolysis of alkoxy groups of TEOS. Besides, the FT-IR spectrum consists of some peaks located at 1516 cm^{-1} (ν_{as}, –N=N–), 1250 cm^{-1}, 1520 cm^{-1} (ν_s, $-NO_2$), 1148 cm^{-1} (C=S), 1377 cm^{-1} (wagging CH_2), 1728 cm^{-1} (ν_{as}, –C=O), indicating that the silica xerogel networks were composed of Si–O–Si backbones.

Figs. 4 and 5 showed the SEM and TEM micrographs of the prepared polyamide/silica hybrid thin films FB-2 and PB-2. In most cases, surface morphology of materials is of great importance for many technical applications requiring well-defined surfaces or interfaces. No phase separation could be observed from Fig. 4. That is, covalent bonding (Si–O–Si) between the organic and inorganic components enhanced miscibility. They were homogeneously and uniformly dispersed at a molecular level. When the silica content was below 15 wt%, the silica particle size was 50 nm, which was shown in Fig. 5. However, when the silica content was increased to 22.5 wt%, the particle size was increased to 65 nm. The increase in the silica particle size clearly resulted from the increase in the aggregation tendency as the silica content and the silica particle number were increased. These micrographs showed the fine interconnected or co-continuous phases morphology, which improved the efficiency of stress transfer mechanisms between the two components.

An attempt for homogeneity was made to estimate the crystallinity of hybrids by the power XRD measurement. In Fig. 6, the diffraction patterns of FB-2 and PB-2 were featureless, showing only broad amorphous halos at $2\theta = 21.57°$, $22.88°$, respectively, derived from homogeneously silica matrix. This result also indicated that covalent bonding (Si–O–Si) between the organic and inorganic components enhanced miscibility.

The thermal stability data of the hybrid materials, as determined by thermogravimetric analysis (TGA), is shown in Fig. 7. The order of the thermal decomposition temperature (T_d) was FB-2 > PB-2 and another data listed in Table 1. They were all above 500 °C for both the FB and the PB hybrid thin films. It suggested the successful incorporation of the silica moiety in the hybrid materials. The slightly lower decomposition temperatures relative to the pure polyimides were probably due to the low molecular weight of polyimide segments in the hybrid materials. Another possibility was the Si–OH residue groups in hybrid thin films since it increased with the silica content because of the incomplete condensation reaction. The T_g of the hybrid assessed by DSC was also

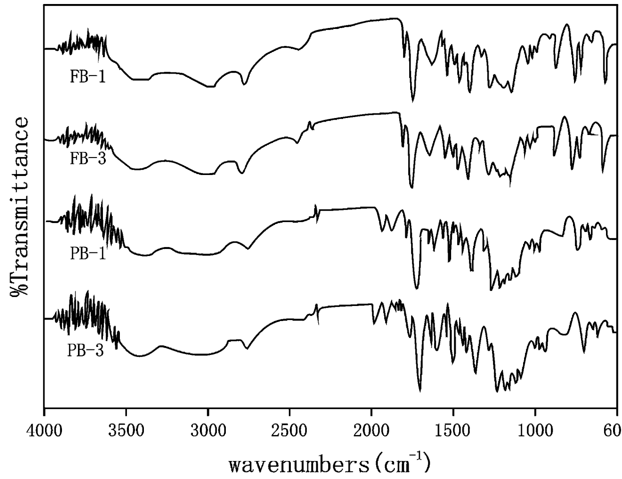

Fig. 3. FT-IR spectrums of hybrid materials.

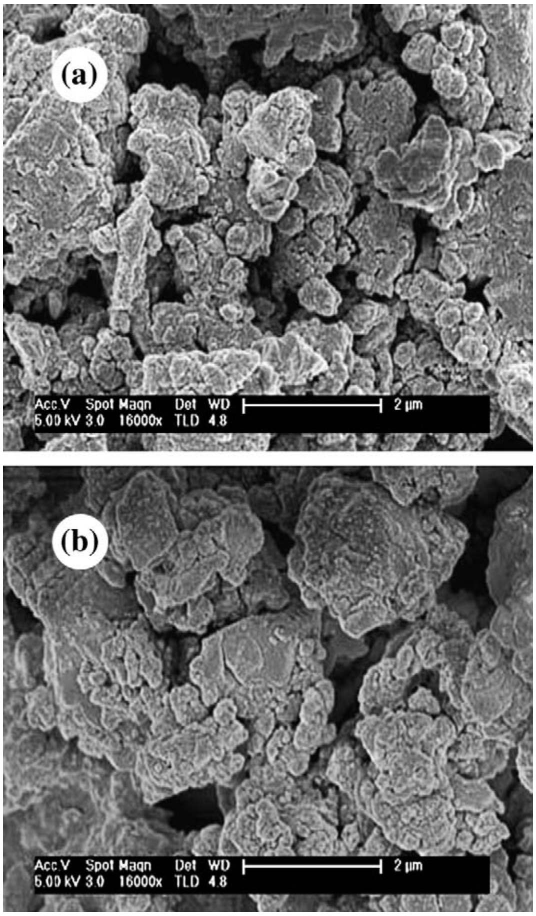

Fig. 4. SEM photographs of FB-2 (a) and PB-2 (b).

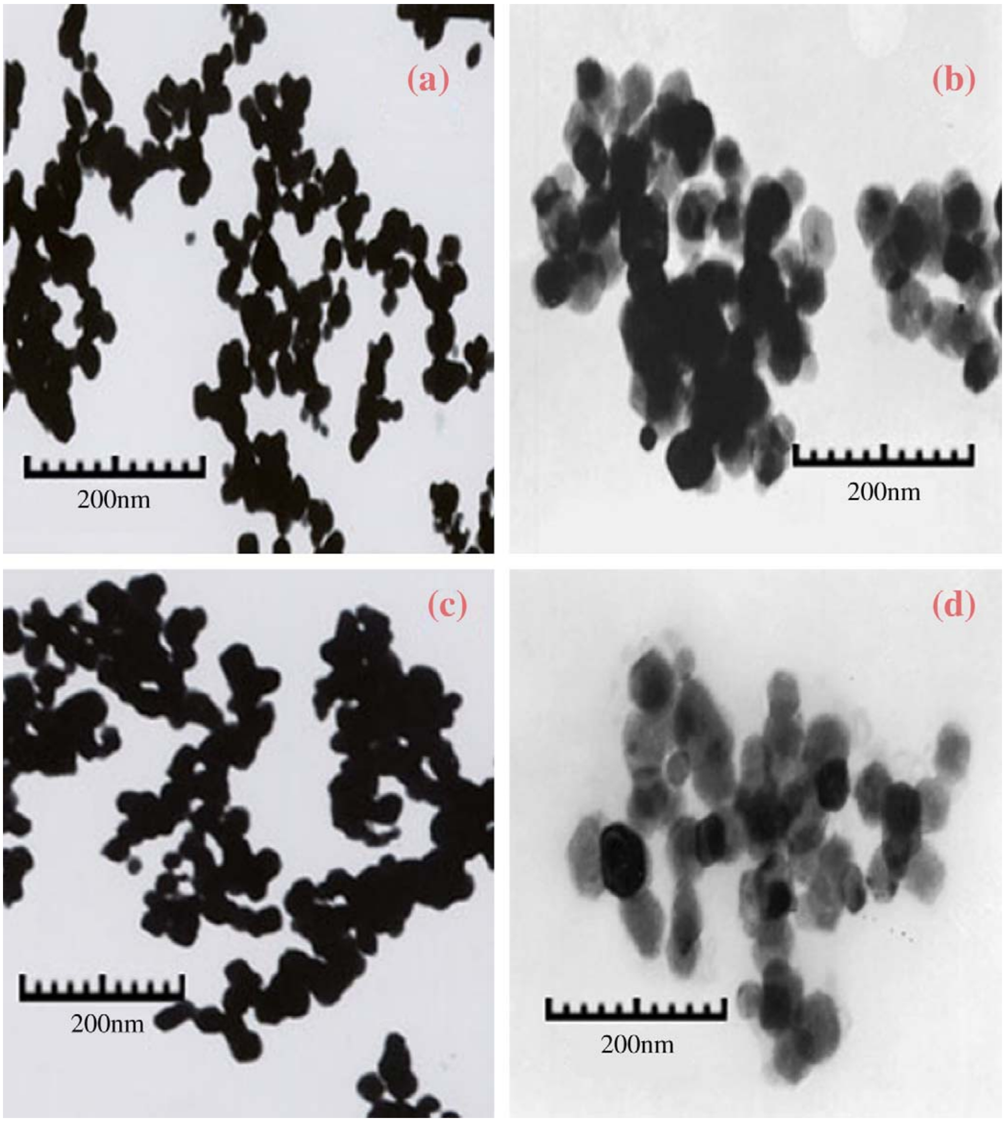

Fig. 5. TEM photographs of FB-2 (a),FB-4 (b), PB-2 (c), and PB-4 (d).

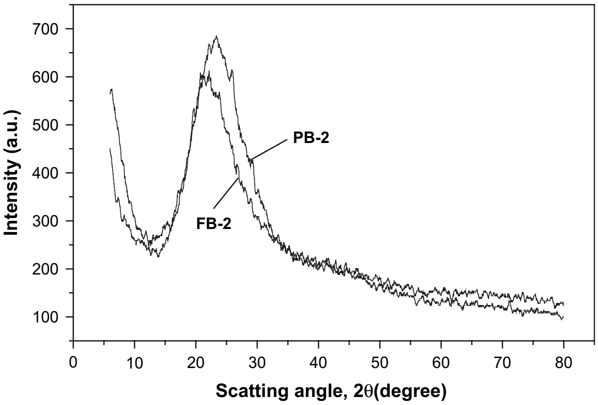

Fig. 6. XRD patterns of the FB-2 and PB-2.

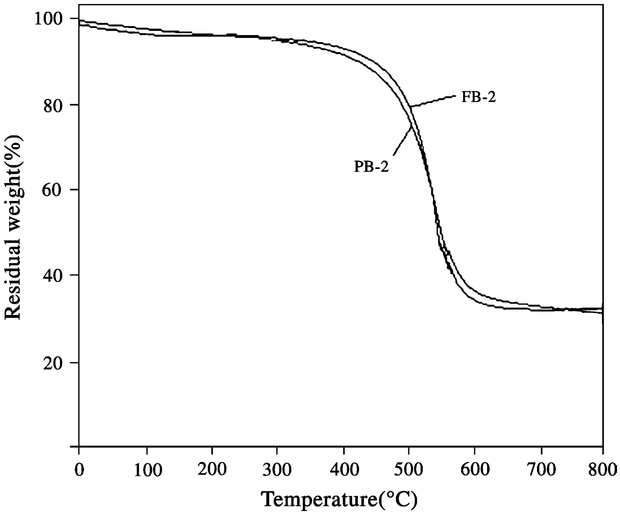

Fig. 7. TGA curves of materials with the heating rate of 10 °C/min under nitrogen.

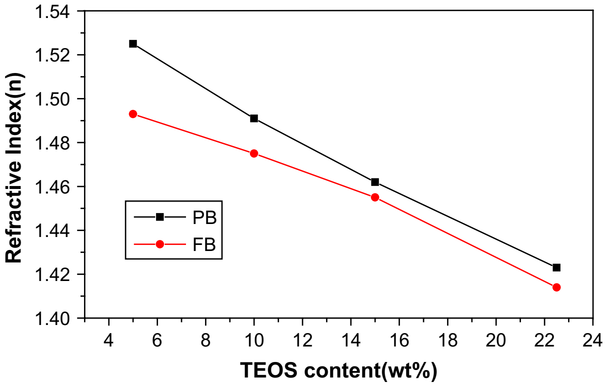

Fig. 8. Variation in the refractive index (at 633 nm) of hybrid thin films with different TEOS content.

slightly increased as the TEOS content was increased (see Table 1). This was clearly caused by the strong interaction between the SiO_2 and the PI, which limited the segmental movement of the PI. It is estimated that these materials will be pretty good for the practical application.

Fig. 8 showed the refractive index (*n*) of the hybrid. The refractive index (*n*) of the prepared hybrid thin films is listed in Table 1. As shown in Table 1, the *n* at 633 nm decreased from 1.525 of PB-1 to 1.423 of PB-4, 1.493 of FB-1 to 1.414 of FB-4, respectively. The *n* could be linearly decreased by increasing the TEOS content, as shown in Fig. 8. It was because of the smaller refractive index of pure silica than the NLO polyimide. The FB series had lower refractive index than PB series, since the introduction of fluoro-containing segment (6FDA) would reduce the refractive index. The result suggested that the *n* of the prepared hybrid thin film could be tunable through the TEOS content. The result suggested that the prepared hybrid thin films had an excellent optical transparency in the UV and visible region (Table 1). According to the Rayleigh equation, the silica particle with a larger size (50 nm) results in a serious light scattering. The particle size of the prepared hybrid films was in the range of 20–50 nm (TEOS content $\leq$ 15 wt%). Therefore, significant scattering loss was avoided. This explained the results of optical transparence (Table 1).

4. Conclusion

Nonlinear optical (NLO) polyimide containing silica inorganic/organic films had been prepared by sol–gel method. Most films were homogeneous and each exhibits good thermal stability. They had network structure and silica particles were uniformly dispersed in the nanoscale. Covalent bonding (Si–O–Si) between the organic and inorganic components enhanced miscibility between the silica and the copolymer. FT-IR, SEM, TEM further confirmed this. The prepared hybrid films showed tunable refractive index with the silica fraction in the films. Excellent optical transparence was obtained in the prepared hybrid films. These results showed that such hybrid thin films had potential applications as passive films for optical devices.

Acknowledgement

This work was financially supported by the Natural Science and advanced technology of Jiangsu Province (BK2003064 & BG 2001034), the National Natural Science Foundation of China (60277020 & 50377005) and the Micro/Nano Science & Technology Fund of Jiangsu University.

References

[1] Rozes L, Noël C, Campistron I, Thomas M, Reyx D, Kajzar F. Macromol Chem Phys 1998;199:2553.
[2] Burland DM, Miller RD, Walsh CA. Chem Rev 1994;94:31.
[3] Briers D, Picard I, Verbiest T, Persoons A, Samyn C. Polymer 2004;45:19.
[4] Singer KD, Sohn JE. Appl Phys Lett 1986;49:248.
[5] Dalton LR, Harper AW, Ghosn R, Steier WH, Ziari M, Fetterman H, et al. Chem Mater 1995;7:1060.
[6] Yang SY, Peng ZH, Yu LP. Macromolecules 1994;27:5858–62.
[7] Wahab MA, Kim Il, Ha CS. Polymer 2003;44:4705.
[8] Qiu WL, Luo YJ, Chen FY. Polymer 2003;44:5821.
[9] Ibanez A, Levy JP, Mouget C, Prieur E. J Solid State Chem 1997;129:22.
[10] Lan T, Kaviratna PD, Pinnavaia TJ. Chem Mater 1994;6:573.
[11] Kioul A, Mascia L. J Non-Cryst Solids 1994;175:169.
[12] Nandi M, Conklin JA, Salvati L, Sen A. Chem Mater 1991;3:201–6.
[13] Wen J, Wilkes GL. Chem Mater 1996;8:1667.
[14] Qiu FX, Zhou YM, Liu JZ. Euro Polym J 2004;40:713–20.
[15] Chen WC, Lee SJ, Lee LH, Lin JL. J Mater Chem 1999;9:2999.
[16] Mascia L, Kioul A. Polymer 1995;36:3649.
[17] Chris J, Cornelius, Marand E. Polymer 2002;43:2385–400.
[18] Tachibana H, Yamanaka Y, Sakai H, Abe M, Matsumoto M. Chem Mater 2000;12:854–6.
[19] Tsai MH, Whang WT. Polymer 2001;42:4197–207.